

A new mouse line reporting the translation of brain-derived neurotrophic factor using green fluorescent protein

<https://doi.org/10.1523/ENEURO.0462-19.2019>

Cite as: eNeuro 2019; 10.1523/ENEURO.0462-19.2019

Received: 5 November 2019

Revised: 11 December 2019

Accepted: 15 December 2019

This Early Release article has been peer-reviewed and accepted, but has not been through the composition and copyediting processes. The final version may differ slightly in style or formatting and will contain links to any extended data.

Alerts: Sign up at www.eneuro.org/alerts to receive customized email alerts when the fully formatted version of this article is published.

Copyright © 2019 Wosnitzka et al.

This is an open-access article distributed under the terms of the Creative Commons Attribution 4.0 International license, which permits unrestricted use, distribution and reproduction in any medium provided that the original work is properly attributed.

1 Title: A new mouse line reporting the translation of brain-derived neurotrophic factor using
2 green fluorescent protein

3
4 Abbreviated title: Quantifying BDNF-translating neurons with GFP

5
6 Author names and affiliations, including postal codes:
7 Erin Wosnitzka, Xinsheng Nan, Jeff Nan, Pedro Chacón-Fernández and Yves-Alain Barde
8 School of Biosciences, Cardiff University CF10 3AX Cardiff United Kingdom

9
10 Lothar Kussmaul, Michael Schuler and Bastian Hengerer
11 Boehringer-Ingelheim, Birkendorfer Str. 65, 88397 Biberach an der Riß, Germany

12
13 Corresponding author email address: bardey@cardiff.ac.uk

14 Number of pages: 14

15 Number of figures: 5

16 1 table

17
18 Number of words for Abstract 209 Introduction 430 and Discussion 879

19
20 The authors declare no conflict of interest

21
22 Acknowledgments: This work was supported by the Sêr Cymru programme, by the NMHRI
23 PhD programme at Cardiff University and by Boehringer-Ingelheim

24

25 **A new mouse line reporting the translation of brain-derived neurotrophic factor using green**
 26 **fluorescent protein**

27 Abbreviated title: Quantifying BDNF-translating neurons with GFP

28 Erin Wosnitzka^{1*}, Xinsheng Nan^{1*}, Jeff Nan¹, Pedro Chacón-Fernández³, Lothar Kussmaul², Michael
 29 Schuler², Bastian Hengerer² and Yves-Alain Barde¹

30 ¹School of Biosciences, Cardiff University, CF10 3AX Cardiff, UK

31 ²Boehringer-Ingelheim, Birkendorfer Str. 65, 88397 Biberach an der Riß, Germany

32 ³Present address: Hospital Universitario Virgen Macarena-FISEVI, University of Seville, E41009
 33 Seville, Spain

34 *These authors contributed equally

36 **Abstract**

37 Whilst BDNF is receiving considerable attention for its role in synaptic plasticity and in nervous
 38 system dysfunction, identifying brain circuits involving BDNF-expressing neurons has been
 39 challenging. BDNF levels are very low in most brain areas, except for the large mossy fibre terminals
 40 in the hippocampus where BDNF accumulates at readily detectable levels. This report describes the
 41 generation of a mouse line allowing the detection of single brain cells synthesising BDNF. A
 42 bicistronic construct encoding BDNF tagged with a P2A sequence preceding GFP allows the
 43 translation of BDNF and GFP as separate proteins. Following its validation with transfected cells this
 44 construct was used to replace the endogenous *Bdnf* gene. Viable and fertile homozygote animals
 45 were generated, with the GFP signal marking neuronal cell bodies translating the *Bdnf* mRNA.
 46 Importantly, the distribution of immunoreactive BDNF remained unchanged as exemplified by its
 47 accumulation in mossy fibre terminals in the transgenic animals. GFP-labelled neurons could be
 48 readily visualised in distinct layers in the cerebral cortex where BDNF has been difficult to detect
 49 with currently available reagents. In the hippocampal formation, quantification of the GFP signal
 50 revealed that fewer than 10% of the neurons do not translate the *Bdnf* mRNA at detectable levels,
 51 with the highest proportion of strongly labelled neurons found in CA3.

52 **Significance statement**

53 BDNF is a highly conserved growth factor known to be essential for the function of the nervous
 54 system. Its very low abundance in the brain has retarded the development of drugs targeting BDNF-
 55 expressing neurons in disease-relevant brain areas. The present report describes a novel approach
 56 allowing the localisation of single cells in the adult mouse brain actively translating *Bdnf* mRNAs
 57 using GFP as a surrogate marker. The availability of these transgenic animals will also help in
 58 understanding the action of drugs such as ketamine thought to act by increasing *Bdnf* translation.

60 **Introduction**

61 Brain-derived neurotrophic factor (BDNF) is a secreted growth factor required for the development
 62 and function of the nervous system (Mitre et al., 2017). In humans, decreased levels of BDNF have
 63 been associated with a wide range of conditions including neurodegeneration (Mariga et al., 2017).
 64 In addition, there is considerable evidence for a role of BDNF in depression (Castren and Kojima,
 65 2017) and memory (Egan et al., 2003; Heldt et al., 2007). There are large differences in the levels of

Bdnf transcription between different brain regions and from one neuron to the next as long documented by *in situ* hybridisation studies in the adult brain of mice, rats and pigs (Hofer et al., 1990; Wetmore et al., 1990). Given that *Bdnf* transcription is regulated by neuronal activity in excitatory neurons (Tao et al., 1998), different degrees of activity most likely contribute to these differences. However, comparisons between the staining intensity of BDNF with surrogate markers of activity such as Arc (Dieni et al., 2012; Nikolaïenko et al., 2018) suggest that other determinants are also likely to play a role. In order to better understand the mechanisms regulating the translation of *BDNF* and to facilitate the development of new drugs targeting BDNF-expressing neurons, it is desirable to use approaches allowing the characterisation of single cells as a function of the intensity of a reporter signal such as GFP. Feasibility is suggested by previous work using vectors encoding *Bdnf*'s regulatory sequences to drive the expression of reporters including GFP (Guillemot et al., 2007; Koppel et al., 2009; Fukuchi et al., 2017). In addition, detectable levels of fluorescence have been illustrated using sequences encoding fluorescent proteins inserted within activity-dependent exons of *Bdnf* (Singer et al., 2018). These previous results indicate that the strength of the *Bdnf* promoters drives levels of GFP expression sufficient to allow single cell visualisation and sorting. Here we report on the substitution of the *Bdnf* gene by a construct containing a bicistronic mRNA encoding *Bdnf* and *Gfp* separated by a short sequence designated P2A previously shown to prevent the elongation of the peptide chain (Szymczak et al., 2004). Fertile homozygote animals were generated using this construct to replace the *Bdnf* coding sequence. Brain sections of the corresponding transgenic animals revealed marked differences in the levels of GFP expression between neurons. The results are discussed in the context of a recent report describing the generation of mouse line with the *Bdnf* gene replaced by a construct encoding a BDNF-GFP fusion protein (Leschik et al., 2019) and of RNA sequencing using single cells isolated from the mouse hippocampus (Habib et al., 2016).

90

91 **Methods**

92 *Constructs, HEK 293 cell culture, transfection and BDNF measurements*

93 Plasmid pCMV6-BDNF was generated by inserting a PCR fragment encoding the full-length mouse
94 BDNF protein into the BamHI site of pCMV6 (Addgene #39857) (Hofer et al., 1990). pCMV-BDNF-myc
95 was constructed by adding one copy of a myc tag at the C-terminus of WT BDNF following deletion
96 of the last 3 amino acids (Matsumoto et al., 2008). To generate BDNF expression constructs
97 containing tandem repeats of myc tags, one SbfI site was first introduced into pCMV-BDNF-myc by
98 PCR followed by inserting multi-copies of myc tags into the SbfI site of the resultant plasmid pCMV-
99 BDNF-myc-SbfI.

100 The following BDNF-GFP and P2A-SV40-NLS-GFP DNA fragments were synthesized at GeneArt
101 (Germany):

102 BDNF-GFP:

103 tttaattaagccaccatgaccatcctgtttctgaccatggtcatcagctacttcggctgcatgaaggccgctcccatgaaggaagtgaacgtgcacg
104 gccagggaacacgtgcttatcctggtgacacacagcaccctggaatctgtgaacggccctagagctggcagcagaggcctgaccacaa
105 caagcctggccgacaccttcgagcacgtgatcgaggaaactgtggacgaggaccagaaagtgcggcccaacgaggaaaaccacaaggacgc
106 cgacctgtacaccagcagagtgtgctgagcagccaggtgccctggaacccctctgtgttctgctggaagagtacaagaactacctggac
107 gccgcaacatgagcatgagagtgcggagacacagcagccagctagaagaggcgagctgagcgtgtgacagcatcagcagtggtgac
108 agccgccgacaagaaaaccgctggacatgtctggcgccacgtgacgtgctggaaaagggtgccagtgccaaggccagctgaagcagt
109 acttctacgagacaaagtgaaccccatgggtacaccaaaggaggctgagaggcatcgacaagagacactggaacagccagtgcagaacc

110 acccagagctacgtgctgggcccgtgacaatggacagcaagaaaagaatcggtgctggcgttcacagaatcgacaccagctgctgtgacccctg
111 accatcaagagaggcagaggaatccggcatggtgtctaagggggaggaaactgttcaccggcgtggtgccatcctggtggaactggatggcgac
112 gtgaacggacacaagttcagcgtgtccggcgaggcggaaggcgacgccacatacggaaagctgacctgaagttcatctgcaccaccggcaa
113 gctgccctgcttggcctaccctcgtgaccacactgacctacggcgtgacgtgcttcagcagataccccgaccatatgaagcagcagcacttctt
114 caagagcgccatgcccagggtctacgtgcaggaaagaaccatcttcttaaggacgacggcaactacaagaccaggcggaagtgaagttcg
115 agggcgacacccctcgtgaacagaatcgagctgaagggtacgtctcaagaggacggcaacatcctgggccacaagctggagtacaactac
116 aacagccacaacgtgtacatcatggccgacaagcagaaaaacggcatcaaagtgaactcaagatccggcacaacatcgaggacggctccgt
117 gcagctggccgaccactaccagcagaacacccctatcggcgacggccctgtgctgctgctgacaaccactacctgagcaccagtcgcccctg
118 agcaaggaccccaacgagaagaggaccacatggtgctgtggaattcgtgaccgctggtgcatcacctgggcatggacgagctgtacaaa
119 tgaggctgccc

120 underlined: PacI, BamHI and Ascl restriction sites

121 P2A-SV40_{NLS}-GFP

122 ggatccggcgccaccaatttcagcctgctgaacaggccggcagctggaagagaaccctggccctcaaagaagagcggaaggtcatggt
123 gtccaaggcgaggaaactgttcaccggcgtggtgccatcctggtggaactggatggcgacgtgaacggccacaagttcagcgtgtccggcga
124 ggcggaaggcgacgccacctatggcaagctgacactgaagttcatctgcaccaccggcaagctgcccgtgcttggcctaccctcgtgacaacc
125 ctgacctacggcgtgacgtcttcagcagataccccgaccacatgaagcagcagcacttctcaagagcgccatgcccagggtctacgtgcagg
126 aacggacatcttcttaaggacgacggcaactacaagaccaggcggaagtgaagttcaggcgataccctcgtgaaccggatcgagctga
127 aggcgatcgactcaagaggacggcaacatcctggccacaagctggagtacaactacaacagccacaacgtgtacatcatggccgacaag
128 cagaaaaacggcatcaaagtgaactcaagatcaggcacaacatcgaggacggctccgtgagctggccgaccactaccagcagaaccccc
129 catcgagatggccccgtgctgctgcccgaaccactacgtgacacagagcgccctgtccaaggaccccaacgagaagaggaccacat
130 ggtgctgctggaattgtgaccgcccgtggcatcacactggcatggacgagctgtacaagtgagctgccc

131 underlined: BamHI and Ascl restriction sites

132 The PacI/Ascl restricted BDNF-GFP fragment was ligated into the identically restricted pAAV plasmid
133 (Kastle et al., 2018). The BDNF-P2A-GFP expression plasmid was generated by exchanging the
134 BamHI-Ascl fragment from the before described plasmid by the BamHI-Ascl gene synthesis fragment
135 containing the teschovirus-1 P2A, the SV40 nuclear localization signal and the GFP coding sequences.

136 The biosynthesis and secretion of tagged BDNF proteins were analysed using HEK 293 cells
137 transfected with plasmids encoding wildtype BDNF, BDNF-GFP, and BDNF-P2A-GFP. The enhanced
138 version of GFP was used throughout. Cultures were maintained in DMEM medium supplemented
139 with 10% FBS, 1% GlutaMAX and 1% non-essential amino acids (NEAAs) (all Gibco). Transfections
140 were performed in a 6-well format using 2 µg of the indicated DNAs combined with 4 µl of
141 Lipofectamine 2000 transfection reagent (Invitrogen) diluted within OptiMEM medium (Gibco). 5-
142 hour after transfection, HEK 293 cells were cultured in N2B27 medium consisting of equal volumes
143 of Neurobasal medium and DMEM-F12 (Gibco), 1% B27 supplement (ThermoFisher Scientific), 1%
144 GlutaMAX and 1% penicillin-streptomycin (penstrep, Gibco). BSA (Sigma-Aldrich) was used at a
145 reduced concentration of 75 µg/ml to facilitate the analysis of the conditioned media by SDS-PAGE.
146 BDNF levels were quantified in conditioned media and brain lysates by ELISA (Naegelin et al., 2018).

147 *Primary neuronal culture and transfection* Cortices of mice at embryonic day 14.5 (E14.5) for
148 transfection and TrkB phosphorylation assays and E17.5 for immunostaining studies were collected
149 in Hank's buffered salt solution (Sigma-Aldrich) and trypsinised in 1 mg/ml Trypsin (Worthington) for
150 20-minute at 37 °C. The reaction was then stopped using 1 mg/ml Trypsin inhibitor (Sigma-Aldrich)
151 before addition of 1 mg/ml DNase I (Thermo Scientific) and gentle dissociation with a 5 ml
152 serological pipette. Cells were then pelleted by centrifugation at 1,400 rpm for 5-minute and re-
153 suspended in DMEM medium supplemented with 2% FBS, 1% GlutaMAX and 1% penstrep. 3-hour

154 after plating into wells coated with poly-d-lysine (Sigma-Aldrich), cells were maintained in
155 Neurobasal medium supplemented with 1% GlutaMAX supplement, 1% penstrep and 2% SM1
156 supplement (Stem Cell Technologies). Neurons were cultured for up to 12 days with 50% media
157 changes performed three-times weekly. Subsequent transfections were performed on E14.5 neurons
158 at 5DIV using 0.5 µg of indicated DNAs and 1 µl Lipofectamine 2000 (see above). Depolarisation of
159 E17.5 neurons at DIV11 was achieved by supplementing media with 1 mM 4-aminopyridine (4-AP)
160 (Merck) for 24-hour.

161 *Imaging and staining of neuronal cultures* 24-hour after transfection or treatment with 4-AP,
162 neurons were briefly washed with PBS and fixed with 4% paraformaldehyde (PFA, Thermo Scientific)
163 for 15-minute. After a 5-minute permeabilisation with PBS containing 0.1% Triton X-100 (Sigma-
164 Aldrich) (PBS-T), cells were incubated for 1-hour in blocking solution (3% donkey serum (Sigma-
165 Aldrich) and 1% BSA in PBS-T) at room temperature (RT). Coverslips were then incubated overnight
166 in primary antibodies diluted in blocking solution at the following concentrations: anti-BDNF mAb#9
167 (7 µg/ml) (Kolbeck et al., 1999), chicken anti-GFP (1:1,000) (Abcam, cat no. ab13970), chicken anti-
168 MAP2 (1:5,000) (Abcam, cat no. ab92434), and rabbit anti-Tau (1:5,000) (Abcam, cat no. ab64193).
169 Following three 5-minute washes in PBS-T, cells were incubated in Alexa Fluor 555 conjugated anti-
170 mouse IgG (Invitrogen, cat no. A-31570), Alexa Fluor 488 conjugated anti-chicken IgY (Invitrogen, cat
171 no. A-11039), Alexa Fluor 647 conjugated anti-chicken IgY (Invitrogen, cat no. A-21449), and Alexa
172 Fluor 647 conjugated anti-rabbit IgG (Invitrogen, cat no. A-21245) secondary antibodies in blocking
173 solution (all at 1:500 dilutions) for 1-hour. After a 5-minute wash with PBS-T, DAPI (Sigma-Aldrich)
174 diluted in PBS (1:4,000) was added to cells for 15-minute. Coverslips were then mounted onto glass
175 slides using Dako fluorescence mounting medium (Agilent). Images were captured using a 63x
176 objective of a confocal microscope and are shown as maximum intensity projections of Z-stack
177 images (LSM 780, Carl Zeiss).

178 *TrkB phosphorylation assay of cultured neurons* The conditioned media of transfected HEK 293 cells
179 transfected with BDNF cDNAs were standardised to a BDNF concentration of 25 ng/ml after
180 quantification using a BDNF ELISA (Naegelin et al., 2018). Before treatment, E14.5 neurons at 5DIV
181 were incubated with fresh media for 15-minute to aid clearance of endogenous phosphorylation.
182 Cells were then incubated with conditioned media containing WT BDNF, or BDNF-P2A for 10-minute.
183 Cells were then washed using PBS supplemented with 2 mM sodium orthovanadate (NaOV) (Sigma-
184 Aldrich) to inhibit phosphatase activity and analysed by SDS-PAGE for TrkB phosphorylation.

185 *Western blot and densitometric analysis* Homogenised brain tissues, HEK 293 cells and cultured
186 neurons were incubated for 20-minute on ice in RIPA buffer (50 mM Tris-HCl, 150 mM NaCl, 1 mM
187 EDTA, 0.1% SDS, 0.2% sodium deoxycholate, and 1% Triton X-100) supplemented with phosphatase
188 and protease inhibitor cocktail mixes, 10 µM phenanthroline monohydrate, 10 mM aminohexanoic
189 acid, 10 µg/ml aprotinin and 2 mM sodium orthovanadate (all Sigma Aldrich). Lysates and
190 conditioned media were centrifuged at 15,000 rpm to remove insoluble components before analysis
191 by SDS-PAGE. Proteins were separated on 4-12% NuPAGE Bis-Tris gels (Invitrogen) and transferred to
192 GE Healthcare Amersham™ Protran NC nitrocellulose membranes (Thermo Scientific) using a Trans-
193 Blot semi-dry transfer unit (Bio-rad). Membranes were subsequently blocked for 1-hour in blocking
194 solution (5% blotting-grade blocker (Biorad) and 1% BSA in TBS containing 0.1% Tween (Sigma-
195 Aldrich) (TBS-T)) and then probed overnight at 4°C with antibodies to beta-actin (Abcam, cat no.
196 ab8229), BDNF (monoclonal 3C11, Icosagen, cat no. 327-100), BDNF propeptide (monoclonal 5H8,
197 Santa Cruz, cat no. sc-65514), GFP (Abcam, cat no. ab13970) or phosphoTrkA (Tyr674/675)/TrkB
198 (Tyr706/707) (Cell Signalling Technology, cat no. 4621) in blocking solution (1:2,000). Following three
199 10-minute washes in TBS-T, membranes were incubated at RT with HRP-conjugated anti-goat (Santa

200 Cruz, cat no. sc-2354), anti-mouse, anti-rabbit (both Promega, cat no. W4021 and W4011
 201 respectively) or anti-chicken (Abcam, cat no. ab6877) secondary antibodies within blocking solution
 202 (1:2,000). After a further three 20-minute washes in TBS-T, membranes were developed using
 203 WesternBright ECL HRP substrate (Advansta). Densitometric analysis of all blots were performed
 204 using quantification functions on Biorad ImageLab software. For blots requiring BDNF quantification,
 205 rBDNF standards (Regeneron/Amgen) between 300 and 18.75 pg were run alongside to create
 206 calibration curves as appropriate.

207 *Animal husbandry and generation of Bdnf-P2a-Gfp animals* All animals in this study were approved
 208 by the Cardiff University Ethical Review Board and all experiments performed within the guidelines
 209 of the Home Office Animals (Scientific Procedures) Act, 1986. *Bdnf* knockout (*Bdnf*^{-/-}) animals were
 210 generated by crossing mice with two floxed *Bdnf* alleles (Rauskolb et al., 2010) with mice expressing
 211 a CMV-Cre transgene (Schwenk et al., 1995). *Bdnf-P2a-Gfp* animals were generated by TACONIC
 212 Biosciences. Briefly, the targeting strategy is based on NCBI transcript NM_001048139.1 and
 213 Ensemble gene ID ENSMUSG00000048482, in which exon 2 contains the complete BDNF coding
 214 sequence. The GSG sequence is then followed by the teschovirus P2A sequence (Liu et al., 2017), the
 215 SV40 nuclear localization sequence (NLS) (Ray et al., 2015) and a GFP sequence inserted between
 216 the last amino acid and the translation termination codon in exon 2 of the BDNF coding sequence.
 217 The presence of the P2A sequence should result in co-translational generation of BDNF and NLS-GFP
 218 proteins. For selection of positively targeted C57BL/6N Tac ES cells, a puromycin selection marker
 219 was flanked by FRT sites and inserted into intron 1. The puromycin selection cassette was deleted in
 220 ES cells by transient expression of Flp recombinase. The remaining FRT recombination site is located
 221 in a non-conserved region of the genome and thus unlikely to interfere with BDNF expression. After
 222 blastocyst injection of targeted ES cells, chimeric animals were bred to C57BL/6N Tac mice to obtain
 223 heterozygous offspring. For colony expansion purposes, heterozygous breeding pairs were set up,
 224 with litters displaying normal Mendelian birth ratios: Amongst 65 animals from 8 litters, the
 225 distribution was as follows: wildtype n = 19, heterozygotes n = 30, and homozygotes n = 16. Animals
 226 of both sexes were used throughout the study and the only sex-related differences illustrated (see
 227 Fig. 3C). After confirming the fertility of homozygotes, the colony was then maintained using a
 228 mixture of breeding pairs. From 3 to 4 weeks of age, animals were housed in mixed genotypes and
 229 were maintained on a 12-hour dark/light cycle, with access to food and water ad-libitum.

230
 231 *Tissue fixation and immunostaining* Three-month old mice killed by pentobarbital injections were
 232 transcardially perfused with ice-cold PBS and 4% paraformaldehyde (PFA), their brains removed and
 233 post-fixed at RT for 4-hour before cryoprotecting in 30% w/v sucrose solution at 4 °C overnight. The
 234 following day, brains were embedded in OCT and sectioned at 40 µm using a cryostat. Sections were
 235 blocked in blocking solution (3% donkey serum and 4% BSA in PBS-T) for 1-hour before incubating
 236 overnight with mouse anti-BDNF (mAb #9) and chicken anti-GFP (1:1,000). Sections were then
 237 washed three times for 10-minute with PBS-T before incubating with Alexa Fluor 555 anti-mouse IgY
 238 and Alexa Fluor 488 anti-chicken IgY secondary antibodies (ThermoFisher Scientific, 1:500) for 1-
 239 hour at RT. After a final wash in PBS-T for 10-minute, sections were incubated with DAPI diluted in
 240 PBS (1:4,000) for 20-minute and mounted onto pre-coated polylysine slides (VWR) with Dako
 241 fluorescence mounting media. Images of gross brain regions were acquired on a confocal
 242 microscope using a 20x objective. For counts of GFP positive nuclei, images were captured using a
 243 63x oil immersion and then analysed using FIJI (Schindelin et al., 2012) and CellProfiler (McQuin et
 244 al., 2018). For each section, masks were created on FIJI to focus automated analyses onto granule
 245 cells of the dentate gyrus (DG) and pyramidal cells of CA1, CA2, and CA3. On CellProfiler, DAPI and
 246 GFP positive nuclei were then identified using individual IdentifyPrimaryObjects modules. GFP
 247 immunostaining was measured using MeasureObjectIntensity, and identified nuclei were

248 categorised using custom-defined bins according to their staining intensity (under categories 'Below
249 Threshold', 'Light', 'Moderate', 'Heavy' or 'Very Heavy').

250 *Statistical analysis.* Data were analysed using Microsoft Excel 2013 and RStudio software. For
251 analysis of *Bdnf-P2a-Gfp* bodyweights, a Kruskal-Wallis test was used with a Conover-Iman post-hoc
252 test for multiple comparisons. TrkB activation by BDNF-fusion proteins was compared against that of
253 BDNF-myc and analysed using a one-sample *t* test. An adjusted *p* value (≤ 0.0125) was considered
254 significant after a Bonferroni-correction for multiple comparisons. Differences in BDNF and GFP
255 signal intensities in depolarised *Bdnf-P2a-Gfp* neurons were analysed using a Student's *t* test. All
256 results were expressed as the mean \pm standard error, and $p \leq 0.05$ was considered significant unless
257 otherwise stated.

258

259 Results

260 *In vitro* experiments with transfected cells

261 As the biosynthesis and secretion of biologically active BDNF is a prerequisite for the generation of
262 viable animals, the suitability of candidate *Bdnf* constructs was first tested using transfected HEK 293
263 cells. Constructs encoding unmodified BDNF, BDNF directly fused with GFP or separated from BDNF
264 by a P2A sequence (Fig. 1A) were introduced into expression vectors and used to transfect HEK 293
265 cells with Lipofectamine. The GFP sequence adds 238 amino acids to the carboxy terminal of the
266 BDNF whilst P2A adds 22 amino acids. Both cell lysates and conditioned media were collected and
267 probed with the BDNF monoclonal antibody 3C11. This antibody unambiguously identifies BDNF in
268 Western blot as demonstrated by the absence of signal in lysates prepared from the cerebral cortex
269 of *Bdnf*^{-/-} animals (Fig. 1B). In transfected cells, unlike is the case with neurons expressing
270 endogenous *Bdnf* (Matsumoto et al., 2008), a significant proportion of the immunoreactive material
271 in cell lysates migrates as pro-BDNF identified using the pro-BDNF antibody 5H8 (data not shown)
272 that can also be detected in the conditioned medium (Fig. 1C). In cell lysates of cells transfected with
273 BDNF-GFP constructs, significant levels of pro-BDNF-GFP can be detected with the anti-BDNF
274 antibody, whilst BDNF-GFP is barely detectable in the conditioned medium (Fig. 1D). By contrast, the
275 bulk of pro-BDNF-P2A is clearly separated from BDNF-P2A and both are readily detectable in the
276 conditioned medium (Fig. 1C). The upward shift of BDNF-P2A compared with recombinant BDNF
277 indicates that the P2A sequence remains attached to BDNF (Fig. 1C). Cell lysates probed with GFP-
278 antibodies confirm the biosynthesis of BDNF and GFP as separate products when encoded by the
279 BDNF-P2A-GFP construct, unlike is the case for the BDNF-GFP fusion construct, with the bulk of the
280 immunoreactive material detected as unprocessed pro-BDNF-GFP (Fig. 1D).

281 As transfected HEK 293 cells do not have a dedicated secretory pathway comparable to neurons, the
282 same three constructs were also used to transfect cultured cortical neurons (Fig. 2). The wild-type
283 (WT) BDNF expression constructs revealed intense staining of neuronal cell bodies as well as dotted
284 staining of MAP2-positive processes (Fig. 2A). With BDNF-GFP constructs, a GFP signal was observed
285 throughout the transfected neurons with the GFP signal partially overlapping with the BDNF
286 immunoreactive signal (Fig. 2B, arrowheads), possibly indicating that a fraction of GFP separates
287 from BDNF (see Discussion). Neurons transfected with the BDNF-P2A constructs revealed a GFP
288 signal largely overlapping with the nucleus, confirming the biosynthesis of BDNF and GFP as separate
289 products in transfected neurons (Fig. 2C).

290 Characterisation of transgenic animals carrying the *Bdnf-P2a-Gfp* replacement construct

291 Having established the suitability of the BDNF-P2A-GFP construct with regard to the biosynthesis and
 292 secretion of BDNF as well as the biosynthesis of BDNF and GFP as distinct products, this construct
 293 was then used to replace the protein-coding region of the endogenous *Bdnf* gene. Following mating
 294 of heterozygote animals, homozygote animals carrying the *Bdnf-P2a-Gfp* construct were born at the
 295 expected Mendelian ratio (see Methods). In addition, the transgene did not measurably interfere
 296 with the fertility of the animals. Coronal brain sections of homozygous animals were then examined
 297 by confocal microscopy following perfusion, fixation and staining with antibodies to GFP, BDNF, as
 298 well as nuclear staining with DAPI (Fig. 3A). The distribution of the BDNF signal is in line with
 299 previous BDNF staining experiments using BDNF antibodies (Conner et al., 1997; Yan et al., 1997;
 300 Dieni et al., 2012) whilst the distribution of the GFP signal corresponds to the results of previous *in*
 301 *situ* hybridisation studies (see also Allen brain atlas, [http://mouse.brain-](http://mouse.brain-map.org/gene/show/11850)
 302 [map.org/gene/show/11850](http://mouse.brain-map.org/gene/show/11850)). Selective GFP labelling can be readily observed in distinct cortical
 303 layers, including layers 2, 5 and 6 as well as in distinct nuclei including the amygdala as well as all
 304 sub-divisions of the hippocampal formation (Fig. 3 A,B). Quantification of the GFP signal using
 305 CellProfiler (Methods) revealed that the vast majority of hippocampal neurons translate the
 306 construct at readily detectable, albeit different levels, with the largest number of heavily labelled
 307 cells found in CA3 and the highest proportion of weakly labelled cells in CA2, CA1 and in the dentate
 308 gyrus (Table 1). We also monitored the postnatal weight gain of the *Bdnf-P2a-Gfp* animals and
 309 observed that starting at about 6 months, homozygote animals gained more weight than their wild-
 310 type littermates, a trend that was even visible in male heterozygotes (Fig. 3C). As the literature
 311 indicates that BDNF levels and TrkB signalling are critical in the regulation of food intake (Lyons et
 312 al., 1999; KERNIE et al., 2000), both in mice and humans (Yeo et al., 2004), we quantified BDNF levels
 313 by ELISA in the cerebral cortex of *Bdnf-P2a-Gfp* animals and found them unchanged compared with
 314 age-matched controls: 35.5 ng/g \pm 2.11 (SEM) WT cortex and 45.4 ng/g \pm 6.38 (SEM) for homozygote
 315 *Bdnf-P2a-Gfp* animals. The corresponding values for the hippocampus were 97.4 ng/g \pm 6.00 (SEM)
 316 and 109.3 ng/g \pm 17.11 (SEM) for WT and homozygous animals respectively. To confirm that GFP is
 317 cleaved after the BDNF-P2A sequence *in vivo*, we analysed the lysates of cortices from wild-type,
 318 heterozygote and *Bdnf-P2a-Gfp* homozygote animals by Western Blot (Fig. 3D). These experiments
 319 revealed a quantitative upward shift of BDNF-P2A compared with the endogenous protein.

320 **TrkB activation by tagged BDNF**

321 Given the lack of evidence for abnormal processing, levels and distribution of BDNF in cells and mice
 322 expressing the *Bdnf-P2a-Gfp* construct, we then asked whether the length of the P2A tag added to
 323 BDNF may compromise its ability to fully activate the BDNF receptor TrkB on neurons, thus
 324 conceivably explaining the abnormal weight gain of adult animals. This hypothesis was tested using
 325 BDNF constructs carrying repeats of a 10-amino acid myc tag used to transfect HEK 293 cells. The
 326 choice of the myc tag for these experiments was inspired by previous studies indicating that the
 327 substitution of *Bdnf* by *Bdnf-Myc* allows the generation of animals with no overt phenotypes
 328 (Matsumoto et al., 2008; Dieni et al., 2012). The biosynthesis and secretion of BDNF was assessed in
 329 cell lysates and conditioned media using the BDNF antibody 3C11 and neither the biosynthesis nor
 330 the secretion of BDNF carrying up to 4myc tags seemed to be compromised (Fig. 4A). The
 331 conditioned media were also used to test the ability of BDNF-myc to trigger TrkB phosphorylation
 332 (Fig. 4B). Primary cultures of mouse cortical neurons were exposed to HEK 293 cell-conditioned
 333 media with their concentrations adjusted to correspond to 25 ng/ml BDNF as determined by ELISA.
 334 The conditioned media of HEK 293 cells transfected with a BDNF-P2A-GFP construct was used in
 335 parallel (Fig. 4B). These experiments revealed that the ability of BDNF-3myc and especially of BDNF-
 336 4myc constructs to activate TrkB was reduced (Fig. 4B).

Localisation and quantification of BDNF and GFP in cultured neurons after depolarisation

Having established the localisation of the BDNF signal and the segregation from the GFP signal in transfected neurons (Fig. 2C), it was of interest to compare these results with those obtained with neurons obtained from the *Bdnf-P2a-Gfp* mouse. As illustrated in Fig. 5, the results are indistinguishable from those obtained with wild-type neurons stained with BDNF antibodies, indicating that the P2A tag does not significantly interfere with the distribution of BDNF. In order to test whether the intensity of the GFP signal is proportional to the BDNF immunoreactive signal, both were quantified before and after depolarisation with 1 mM 4-AP. Both signals were found to increase by more than two-fold after 24-hour (Fig. 5).

Discussion

The main conclusion of this study is that GFP can be used as a surrogate marker to identify cells translating the *Bdnf* mRNA in the adult mouse brain. The results also indicate that the GFP signal intensity is proportional to the degree of BDNF translation as revealed by experiments with cultured neurons. Whilst BDNF and GFP are obviously very different proteins with different half-lives, GFP is mostly targeted to the nucleus whereas BDNF accumulates in vesicles. This differential sub-cellular localisation may explain why the relative signal intensities after acute depolarisation do not perfectly match quantitatively (Fig. 5). In the brain, the distribution of the GFP is in remarkable agreement with the known distribution of the *Bdnf* signal observed in previous *in situ* hybridisation studies, including the Allen brain atlas (<http://mouse.brain-map.org/gene/show/11850>). Importantly, the distribution of the endogenous BDNF protein remains unchanged when comparing the staining of BDNF in the hippocampal formation (Fig. 3A) with previous results using antibodies to myc- or hemagglutinin-tagged versions of the *Bdnf* gene (Matsumoto et al., 2008; Yang et al., 2009). This distribution is also in agreement with results obtained with rat brain sections with the then available, validated BDNF polyclonal antibodies (Conner et al., 1997; Yan et al., 1997). The fact that neither the viability of homozygote animals nor their fertility are compromised further suggests that BDNF-dependent circuits are likely to remain functional. However, the *Bdnf-P2a-Gfp* mice do abnormally gain weight several months after birth, especially in males, suggesting that these animals may be best investigated as young adults in future studies. As the BDNF levels are unchanged in these animals (see Results and Fig. 1B), it is conceivable that the 22-amino acid tag attached to the carboxy terminal of BDNF may chronically reduce TrkB activation *in vivo*, thus potentially explaining the progressive weight gain that is apparent in male animals at about 6 months of ages. Sub-maximal activation of TrkB over extended periods of time *in vivo* may impair the functionality of the circuitry involved in the feeding behaviour of the transgenic animals. These results also suggest that there is only limited scope to add extended tags to BDNF while fully preserving biological activity. In particular, TrkB activation with the 4-myc tag construct (adding 40 amino acids) is reduced by about 50%. Caution should then be exerted when using comparatively large fusion constructs such as BDNF-GFP as they would seem unlikely to efficiently activate TrkB. The results presented in Fig. 1 also indicate additional problems with the processing of pro-BDNF-GFP and the secretion of BDNF-GFP is barely detectable in the conditioned medium of HEK 293 cells transfected with BDNF-GFP constructs (Fig. 1). This conclusion contrasts with the results detailed in a recent, closely related study on *Bdnf* gene substitution with GFP directly coupled to the carboxy terminal of BDNF (Leschik et al., 2019). This gene replacement strategy led to a decrease of about 50% of the expected Mendelian ratio of animals homozygote for the replacement of *Bdnf* by *Bdnf-Gfp*. In addition, the distribution of the GFP signal in these animals does not report the distribution of the endogenous BDNF protein as exemplified by the lack of enrichment of the GFP signal in mossy fibre terminals

(see above). It is conceivable that GFP may have been cleaved from BDNF in the surviving animals as a functional cleavage site at the carboxy terminal of BDNF has been noted following the isolation of BDNF from brain homogenates (Rodriguez-Tebar et al., 1991). However, it should also be noted that this tentative explanation does not account for the Western blot results included in the study by Leschik and colleagues (see Leschik et al., 2019).

The approach described here now opens the possibility to use the GFP signal to isolate and sort cells from the adult brain based on GFP signal intensity, thus allowing their individual profiling by RNAseq. Such results would help informing the development of drugs selectively targeting these neurons and may deliver new clues as to endogenous regulators of BDNF expression. Similar objectives could in principle also be reached by randomly isolating single cells from brain regions of interest without prior cell marking. As such data are indeed available for the adult mouse hippocampus (Habib et al., 2016), we compared them with those reported here. The main outcome of this comparison is that the hierarchy is somewhat different from what can be inferred from *Bdnf* mRNA levels. In particular, the study by Habib et al. indicates that the dentate gyrus contains the highest number of cells containing *Bdnf* mRNA (see *Bdnf* in https://portals.broadinstitute.org/single_cell/study/SCP1/-single-nucleus-rna-seq-of-cell-diversity-in-the-adult-mouse-hippocampus-snuc-seq#study-visualize), possibly due to the selective inclusion of DAPI-positive cells in the granule cell and pyramidal cell layer. We also note that the results summarised in Table 1 closely match previous *in situ* hybridisation studies in the rat (Conner et al., 1997) and the mouse (see e.g. <http://mouse.brain-map.org/gene/show/11850>).

In conclusion, the mouse line reported in this study should facilitate the detailed characterisation of brain neurons actively translating the *Bdnf* mRNA by allowing the selection of cells based on the intensity of the GFP signal. This should prove useful towards the development of new drugs aiming at selectively increasing the levels of BDNF in brain regions of interest, including rapidly acting depressants such as ketamine thought to act by increasing BDNF translation (Bjorkholm and Monteggia, 2016).

References

- Bjorkholm C, Monteggia LM (2016) BDNF - a key transducer of antidepressant effects. *Neuropharmacology* 102:72-79.
- Castren E, Kojima M (2017) Brain-derived neurotrophic factor in mood disorders and antidepressant treatments. *Neurobiol Dis* 97:119-126.
- Conner JM, Lauterborn JC, Yan Q, Gall CM, Varon S (1997) Distribution of brain-derived neurotrophic factor (BDNF) protein and mRNA in the normal adult rat CNS: evidence for anterograde axonal transport. *J Neurosci* 17:2295-2313.
- Dieni S, Matsumoto T, Dekkers M, Rauskolb S, Ionescu MS, Deogracias R, Gundelfinger ED, Kojima M, Nestel S, Frotscher M, Barde YA (2012) BDNF and its pro-peptide are stored in presynaptic dense core vesicles in brain neurons. *J Cell Biol* 196:775-788.
- Egan MF, Kojima M, Callicott JH, Goldberg TE, Kolachana BS, Bertolino A, Zaitsev E, Gold B, Goldman D, Dean M, Lu B, Weinberger DR (2003) The BDNF val66met polymorphism affects activity-dependent secretion of BDNF and human memory and hippocampal function. *Cell* 112:257-269.
- Fukuchi M, Izumi H, Mori H, Kiyama M, Otsuka S, Maki S, Maehata Y, Tabuchi A, Tsuda M (2017) Visualizing changes in brain-derived neurotrophic factor (BDNF) expression using bioluminescence imaging in living mice. *Sci Rep* 7:4949.
- Guillemot F, Cerutti I, Auffray C, Devignes MD (2007) A transgenic mouse model engineered to investigate human brain-derived neurotrophic factor in vivo. *Transgenic Res* 16:223-237.

- 429 Habib N, Li Y, Heidenreich M, Swiech L, Avraham-Davidi I, Trombetta JJ, Hession C, Zhang F, Regev A
430 (2016) Div-Seq: Single-nucleus RNA-Seq reveals dynamics of rare adult newborn neurons.
431 Science 353:925-928.
- 432 Heldt SA, Stanek L, Chhatwal JP, Ressler KJ (2007) Hippocampus-specific deletion of BDNF in adult
433 mice impairs spatial memory and extinction of aversive memories. Mol Psychiatry 12:656-
434 670.
- 435 Hofer M, Pagliusi SR, Hohn A, Leibrock J, Barde YA (1990) Regional distribution of brain-derived
436 neurotrophic factor mRNA in the adult mouse brain. EMBO J 9:2459-2464.
- 437 Kastle M, Kistler B, Lamla T, Bretschneider T, Lamb D, Nicklin P, Wyatt D (2018) FKBP51 modulates
438 steroid sensitivity and NFkappaB signalling: A novel anti-inflammatory drug target. Eur J
439 Immunol 48:1904-1914.
- 440 Kernie SG, Liebl DJ, Parada LF (2000) BDNF regulates eating behavior and locomotor activity in mice.
441 EMBO J 19:1290-1300.
- 442 Kolbeck R, Bartke I, Eberle W, Barde YA (1999) Brain-derived neurotrophic factor levels in the
443 nervous system of wild-type and neurotrophin gene mutant mice. J Neurochem 72:1930-
444 1938.
- 445 Koppel I, Aid-Pavlidis T, Jaanson K, Sepp M, Pruunsild P, Palm K, Timmusk T (2009) Tissue-specific
446 and neural activity-regulated expression of human BDNF gene in BAC transgenic mice. BMC
447 Neurosci 10:68.
- 448 Leschik J, Eckenstaler R, Endres T, Munsch T, Edelmann E, Richter K, Kobler O, Fischer KD,
449 Zuschratter W, Brigadski T, Lutz B, Lessmann V (2019) Prominent Postsynaptic and Dendritic
450 Exocytosis of Endogenous BDNF Vesicles in BDNF-GFP Knock-in Mice. Mol Neurobiol. 56:
451 6833-6855.
- 452 Liu Z, Chen O, Wall JBJ, Zheng M, Zhou Y, Wang L, Ruth Vaseghi H, Qian L, Liu J (2017) Systematic
453 comparison of 2A peptides for cloning multi-genes in a polycistronic vector. Sci Rep 7:2193.
- 454 Lyons WE, Mamounas LA, Ricaurte GA, Coppola V, Reid SW, Bora SH, Wihler C, Koliatsos VE,
455 Tessarollo L (1999) Brain-derived neurotrophic factor-deficient mice develop aggressiveness
456 and hyperphagia in conjunction with brain serotonergic abnormalities. Proc Natl Acad Sci U S
457 A 96:15239-15244.
- 458 Mariga A, Mitre M, Chao MV (2017) Consequences of brain-derived neurotrophic factor withdrawal
459 in CNS neurons and implications in disease. Neurobiol Dis 97:73-79.
- 460 Matsumoto T, Rauskolb S, Polack M, Klose J, Kolbeck R, Korte M, Barde YA (2008) Biosynthesis and
461 processing of endogenous BDNF: CNS neurons store and secrete BDNF, not pro-BDNF. Nat
462 Neurosci 11:131-133.
- 463 McQuin C, Goodman A, Chernyshev V, Kamentsky L, Cimini BA, Karhohs KW, Doan M, Ding L, Rafelski
464 SM, Thirstrup D, Wiegraebe W, Singh S, Becker T, Caicedo JC, Carpenter AE (2018)
465 CellProfiler 3.0: Next-generation image processing for biology. PLoS Biol 16:e2005970.
- 466 Mitre M, Mariga A, Chao MV (2017) Neurotrophin signalling: novel insights into mechanisms and
467 pathophysiology. Clin Sci (Lond) 131:13-23.
- 468 Naegelin Y, Dingsdale H, Sauberli K, Schadelin S, Kappos L, Barde YA (2018) Measuring and Validating
469 the Levels of Brain-Derived Neurotrophic Factor in Human Serum. eNeuro 5. DOI:
470 10.1523/ENEURO.0419-17.2018
- 471 Nikolaenko O, Patil S, Eriksen MS, Bramham CR (2018) Arc protein: a flexible hub for synaptic
472 plasticity and cognition. Semin Cell Dev Biol 77:33-42.
- 473 Rauskolb S, Zagrebelsky M, Dreznjak A, Deogracias R, Matsumoto T, Wiese S, Erne B, Sendtner M,
474 Schaeren-Wiemers N, Korte M, Barde YA (2010) Global deprivation of brain-derived
475 neurotrophic factor in the CNS reveals an area-specific requirement for dendritic growth. J
476 Neurosci 30:1739-1749.
- 477 Ray M, Tang R, Jiang Z, Rotello VM (2015) Quantitative tracking of protein trafficking to the nucleus
478 using cytosolic protein delivery by nanoparticle-stabilized nanocapsules. Bioconjug Chem
479 26:1004-1007.

- 480 Rodriguez-Tebar A, Dechant G, Barde YA (1991) Neurotrophins: structural relatedness and receptor
481 interactions. *Philos Trans R Soc Lond B Biol Sci* 331:255-258.
- 482 Schindelin J, Arganda-Carreras I, Frise E, Kaynig V, Longair M, Pietzsch T, Preibisch S, Rueden C,
483 Saalfeld S, Schmid B, Tinevez JY, White DJ, Hartenstein V, Eliceiri K, Tomancak P, Cardona A
484 (2012) Fiji: an open-source platform for biological-image analysis. *Nat Methods* 9:676-682.
- 485 Schwenk F, Baron U, Rajewsky K (1995) A cre-transgenic mouse strain for the ubiquitous deletion of
486 loxP-flanked gene segments including deletion in germ cells. *Nucleic Acids Res* 23:5080-
487 5081.
- 488 Singer W et al. (2018) BDNF-Live-Exon-Visualization (BLEV) Allows Differential Detection of BDNF
489 Transcripts in vitro and in vivo. *Front Mol Neurosci* 11:325.
- 490 Szymczak AL, Workman CJ, Wang Y, Vignali KM, Dilioglou S, Vanin EF, Vignali DA (2004) Correction of
491 multi-gene deficiency in vivo using a single 'self-cleaving' 2A peptide-based retroviral vector.
492 *Nat Biotechnol* 22:589-594.
- 493 Tao X, Finkbeiner S, Arnold DB, Shaywitz AJ, Greenberg ME (1998) Ca²⁺ influx regulates BDNF
494 transcription by a CREB family transcription factor-dependent mechanism. *Neuron* 20:709-
495 726.
- 496 Wetmore C, Ernfors P, Persson H, Olson L (1990) Localization of brain-derived neurotrophic factor
497 mRNA to neurons in the brain by in situ hybridization. *Exp Neurol* 109:141-152.
- 498 Yan Q, Rosenfeld RD, Matheson CR, Hawkins N, Lopez OT, Bennett L, Welcher AA (1997) Expression
499 of brain-derived neurotrophic factor protein in the adult rat central nervous system.
500 *Neuroscience* 78:431-448.
- 501 Yang J, Siao CJ, Nagappan G, Marinic T, Jing D, McGrath K, Chen ZY, Mark W, Tessarollo L, Lee FS, Lu
502 B, Hempstead BL (2009) Neuronal release of proBDNF. *Nat Neurosci* 12:113-115.
- 503 Yeo GS, Connie Hung CC, Rochford J, Keogh J, Gray J, Sivaramakrishnan S, O'Rahilly S, Farooqi IS
504 (2004) A de novo mutation affecting human TrkB associated with severe obesity and

Region	Proportions of GFP-positive cells				
	Background	Light	Moderate	Heavy	Very heavy
DG	5.37%	55.26%	32.08%	6.66%	0.64%
SEM	1.79%	6.33%	5.05%	2.95%	0.24%
CA1	4.11%	65.43%	24.25%	5.39%	0.81%
SEM	1.33%	7.38%	5.43%	3.47%	0.69%
CA2	5.52%	57.25%	26.69%	9.93%	0.61%
SEM	1.55%	7.65%	4.96%	3.90%	0.26%
CA3	6.96%	31.50%	37.82%	17.58%	6.15%
SEM	0.92%	4.11%	2.05%	2.64%	1.45%

505 developmental delay. *Nat Neurosci* 7:1187-1189.

506

507 Table 1. Quantification of GFP signal intensity in the hippocampal formation

508 The results are based on sections from three different, 3-month-old female homozygous animals.
509 Five sections per animal were used and quantification performed using CellProfiler (Methods).
510 Quantification of the GFP signal was performed by recording the intensity of the Alexa Fluor 488 in
511 sections stained with chicken anti-GFP primary antibody and Alexa Fluor 488 conjugated anti-chicken
512 IgY secondary antibody.

513 DG: Dentate gyrus. Counts were based on DAPI-stained nuclei in the DG granule cell layer and in the
514 pyramidal cell layer for CA1/CA2/CA3. All analysed sections fell between Bregma coordinates -1.355
515 and -2.88.

516

517 Figure legends

518 Figure 1. Constructs, validation of monoclonal antibody 3C11 and transfection of HEK 293 cells 519 with BDNF expression plasmids

520 (A) Schematic representation of BDNF plasmid translation products. (B) Validation of monoclonal
521 antibody 3C11 for BDNF western blot using brain lysates from *Bdnf* wildtype (WT), heterozygous
522 (Het) and knock-out (KO) littermates at postnatal day 7. Western blot analysis of cell lysates and
523 conditioned media using anti-BDNF (mAb 3C11) (C) and anti-GFP (D). Cells were transfected with the
524 indicated plasmids. Note that three-times more conditioned media was loaded into lanes for BDNF-
525 GFP to aid detection of low levels

526 Figure 2. BDNF and GFP localisation in transfected primary neurons.

527 E14.5 cortical cultures at 6DIV transfected with cDNAs encoding WT BDNF (A), BDNF-GFP (B) and
528 BDNF-P2A-GFP (C) and stained using antibodies against BDNF and MAP2. In all transfections, the
529 majority of BDNF immunoreactivity was observed in cell bodies in areas likely corresponding to
530 Golgi. In BDNF-GFP transfected cells (B), separation of GFP fluorescence (green) from BDNF
531 immunofluorescence (magenta) was observed in both the nucleus and proximal neurites (indicated
532 by white arrowheads.

533

534 Figure 3: Characterisation of *Bdnf-P2a-Gfp* mice.

535 (A) Co-staining of BDNF and GFP homozygous *Bdnf-P2a-Gfp* hippocampus. Note the clear separation
536 of GFP and BDNF in the mossy fibre projections of hippocampal CA3. (B) GFP staining of homozygote
537 brains reveals a comparable staining pattern to previous *in situ* hybridisation experiments, with
538 staining in distinct cortical layers, hippocampal formation and amygdala. (C) Body weights of young
539 adult (3-4 months old) and adult (6-7 months old) *Bdnf-P2a-Gfp* mice. Whilst there were no
540 significant differences observed between littermates during young adulthood, significant weight gain
541 could be observed in both heterozygous and homozygous males by 6 - 7 months of age ($p = 0.0100$
542 and $p = 0.0017$ respectively). The bars represent the mean weights \pm standard error, $n \geq 7$ across
543 genotypes and age categories. (D) Western blot analysis of adult *Bdnf-P2a-Gfp* brain lysates. Note
544 the shift in the molecular weight of BDNF after addition of the P2A sequence, and the separation of
545 BDNF-P2A from GFP in *Bdnf-P2a-Gfp* heterozygous (Het) and homozygous (Hom) animals (two
546 animals shown per genotype).

547

548 Figure 4: Increasing the length of BDNF-fusion proteins attenuates their ability to phosphorylate 549 TrkB.

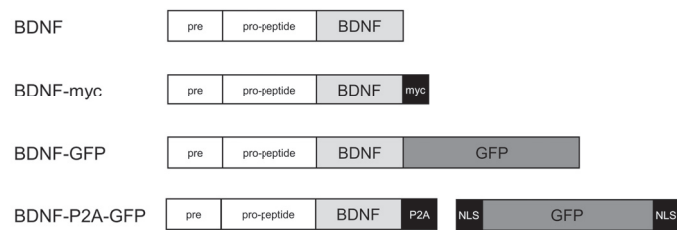
550 (A) Western blot analysis of cell lysates and conditioned media using anti-BDNF (mAb 3C11). Cells
551 were transfected with cDNAs encoding BDNF carrying multiple additions of the 10 amino acid myc
552 tag. (B) TrkB phosphorylation in primary neurons treated with conditioned media containing BDNF
553 fusion proteins standardised to 25 ng/ml. Note that the potency of TrkB phosphorylation is
554 significantly reduced as genetically encoded tags increase in length (BDNF-3myc $p = 0.00312$, BDNF-

4myc $p = 0.00394$). Bars representative of mean relative phosphorylation (compared to BDNF-myc) \pm standard error.

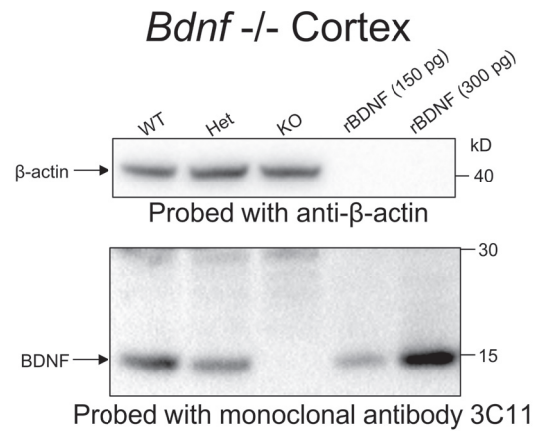
Figure 5: BDNF localisation in wild-type versus homozygous *Bdnf-P2a-Gfp* neurons

Immunostaining of primary neurons with antibodies against BDNF (mAb #9), GFP, and Tau. After 24-hour of treatment with 4-aminopyridine (4-AP), note the increased number of BDNF puncta in neuronal projections and the increased GFP signal intensity in *Bdnf-P2a-Gfp* cultures. Quantification of immunostained *Bdnf-P2a-Gfp* cultures revealed significant increases in both BDNF and GFP following 4-AP treatment. Quantification of immunostained *Bdnf-P2a-Gfp* cultures revealed significant increases in both BDNF and GFP following 4-AP treatment ($p = 3.94 \times 10^{-21}$ and 7.85×10^{-24} respectively. $n = 90$ for both conditions).

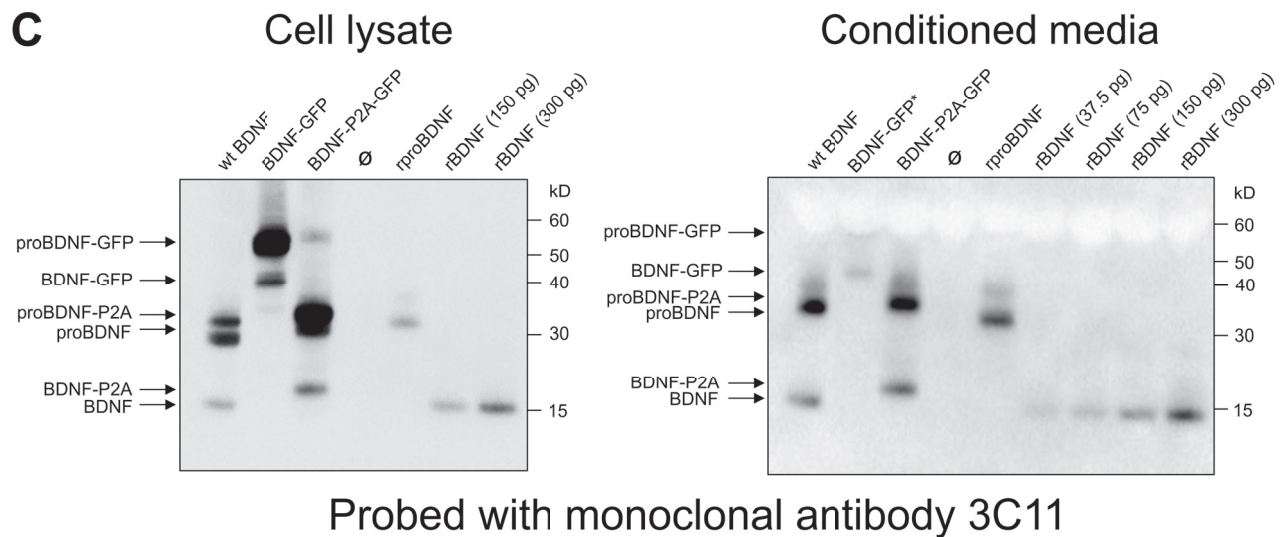
A



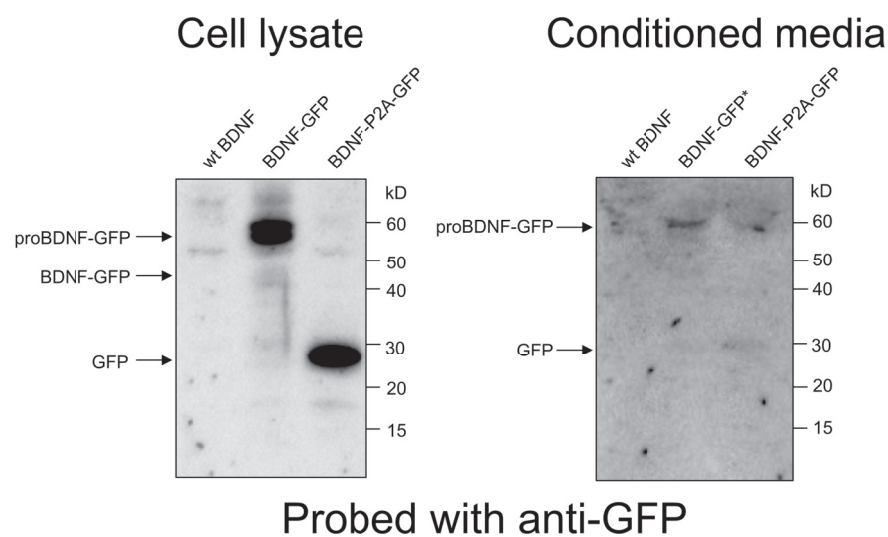
B

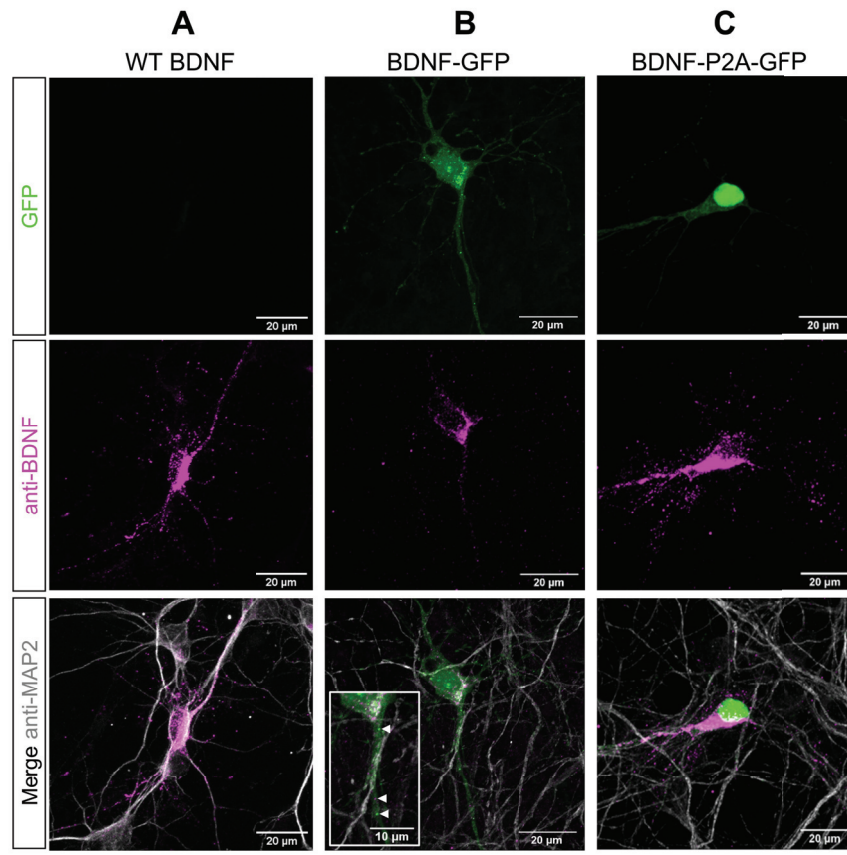


C

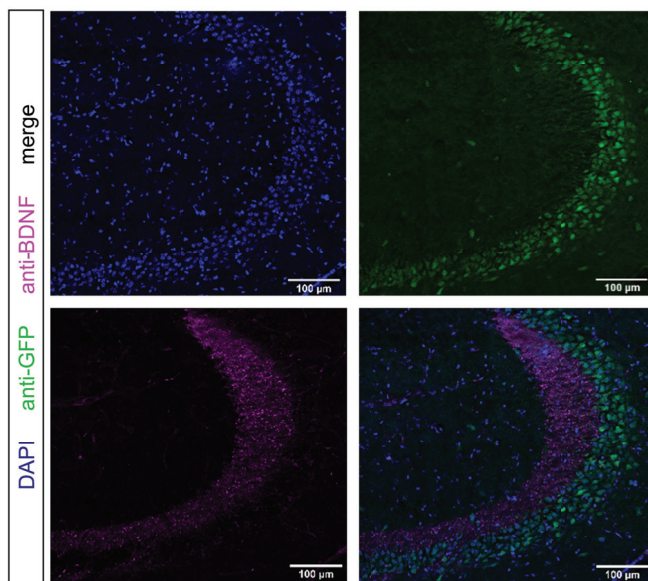


D

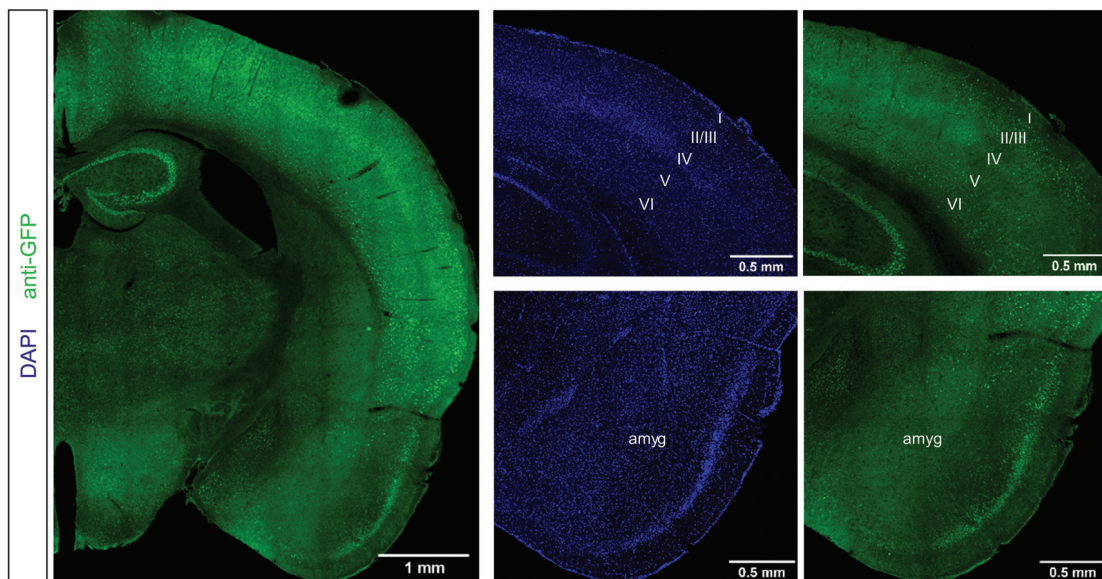




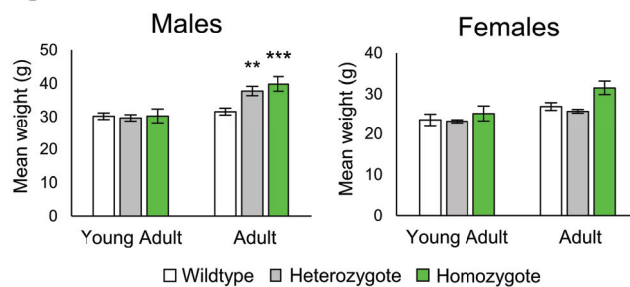
A



B



C



D

